Science Advances
AAAS

Supplementary Materials for

PD-1 independent of PD-L1 ligation promotes glioblastoma growth through the NFκB pathway

Reza Mirzaei, Ashley Gordon, Franz J. Zemp, Mehul Kumar, Susobhan Sarkar, H. Artee Luchman, Anita C. Bellail, Chunhai Hao, Douglas J. Mahoney, Jeff F. Dunn, Pinaki Bose, V. Wee Yong*

*Corresponding author. Email: vyong@ucalgary.ca

Published 5 November 2021, *Sci. Adv.* **7**, eabh2148 (2021)
DOI: 10.1126/sciadv.abh2148

The PDF file includes:

Other Supplementary Material for this manuscript includes the following:

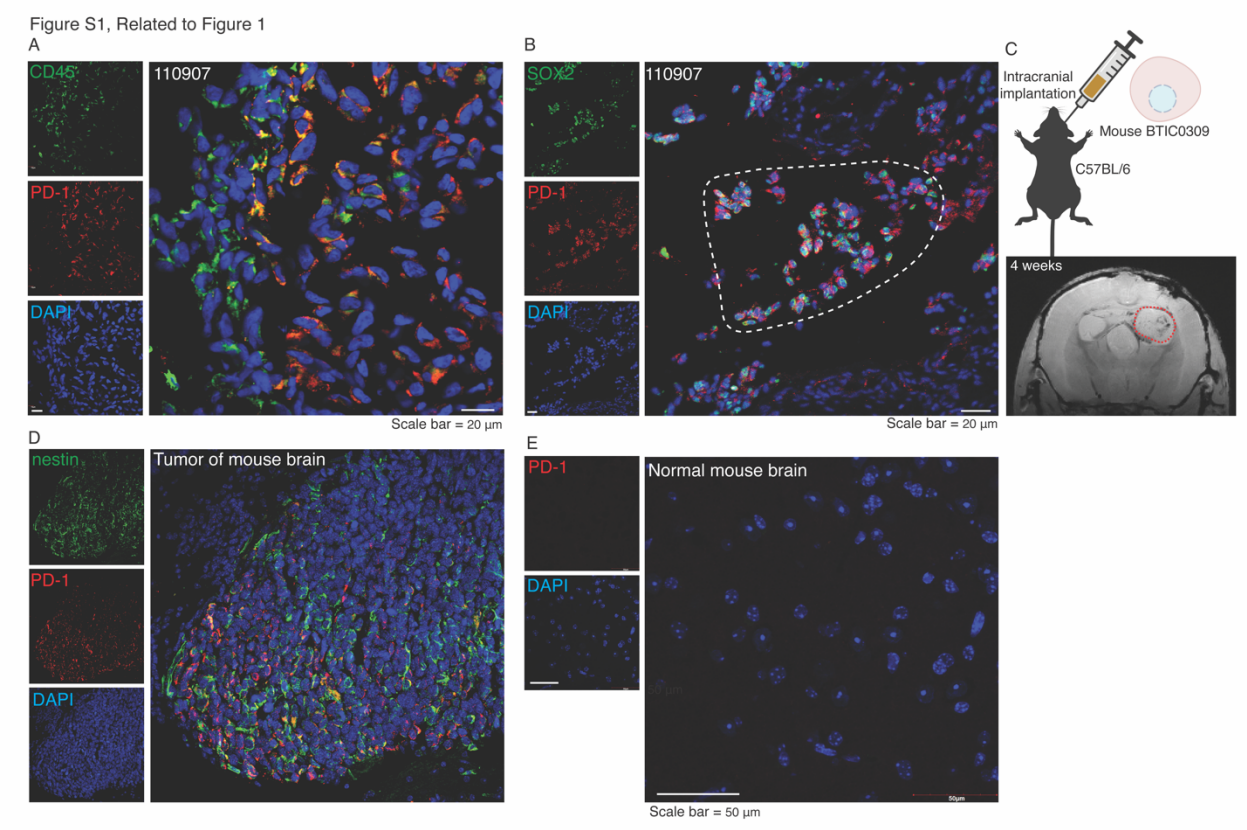

Fig. S1. The expression of PD-1 within the tumor microenvironment of human and mouse model of GBM, Related to Fig. 1. (A) Representative image of immunofluorescence staining of CD45 and PD-1 in tissue sections from human GBM patient 110907. (B) Confirmation of PD-1 expression on SOX2-positive BTICs by immunofluorescence staining of human GBM patient 110907 with a different monoclonal antibody (Clone UMAB199). Dotted outline corresponds to the area where there are PD-1 and SOX2 double positive cells. Nuclei were counterstained with DAPI. (C) Schematic diagram depicts the procedure of mouse intracranial implantation and follow-up magnetic resonance imaging (MRI). (D) Representative images of immunofluorescence staining of BTIC marker nestin, and PD-1 in a section of mouse

tumor. (E) Representative images of immunofluorescence staining of PD-1 in normal brain collected from naïve C57BL/6 mice.

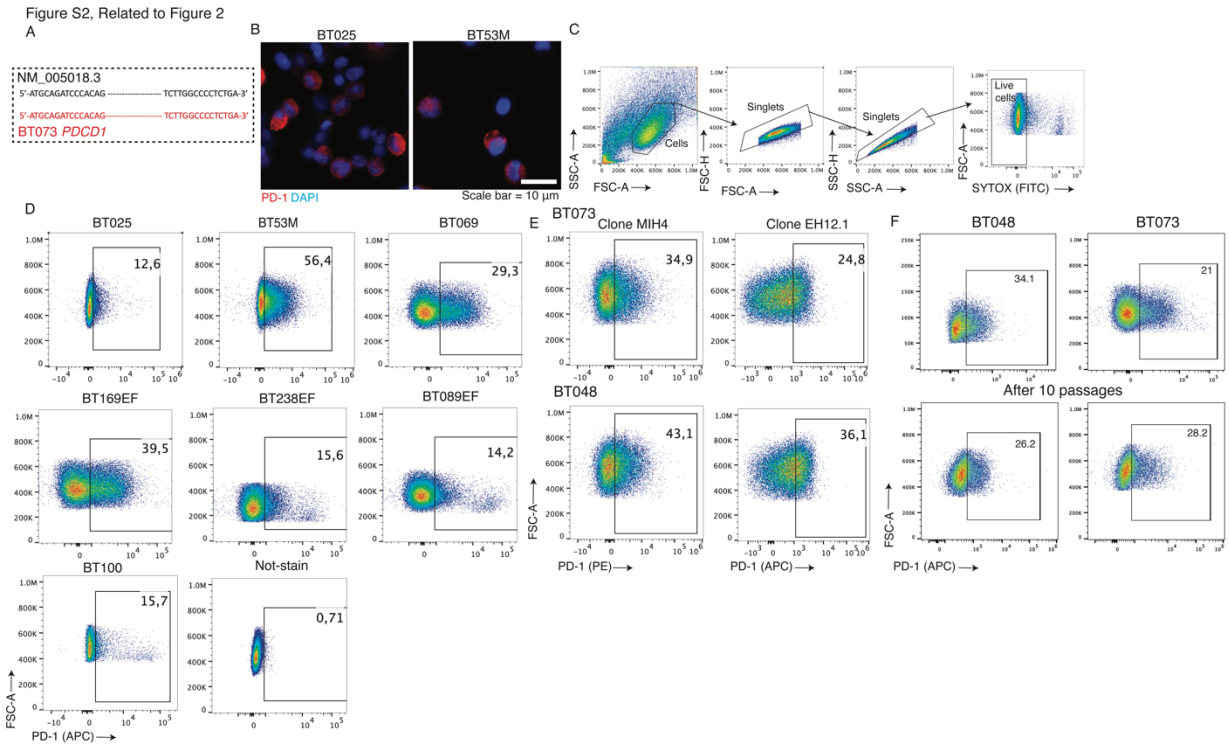

Fig. S2. The expression of PD-1 on human BTICs derived from GBM patients, related to Fig. 2. (A) Alignment of coding sequence (CDS) of *PDCD1* transcripts obtained from human BT073 with the NCBI Reference Sequence: NM_005018.3. Same results were generated for GBM5 and BT025 cell lines (not shown). (B) Representative immunofluorescence images of PD-1 staining of human BT025 and BT53M. Nuclei were counterstained with DAPI. (C) Flow cytometry gating strategy. Forward scatter-versus side scatter-area (FSC-A vs SSC-A) gating was used to identify cells of interest based on size (FSC-A) and granularity (SSC-A) and exclude debris. By using two-step gating of FSC-A vs FSC-height (FSC-H) and SSC-A vs SSC-height (SSC-H), we eliminated doublet cells from our analysis. Finally, dead cells were gated out by staining them with SYTOX green (FITC) nucleic acid stain. (D) Representative flow cytometry plots of surface PD-1 expression on different patient-derived BTIC lines. (E) Flow

cytometry plots of surface PD-1 expression employing two monoclonal antibodies from different clones, MIH4 and EH12.1. (F) Flow cytometry analysis of PD-1 expression on BT048 and BT073 before and after 10 passages in culture. All images and graphs representative of 2-3 independent experiments.

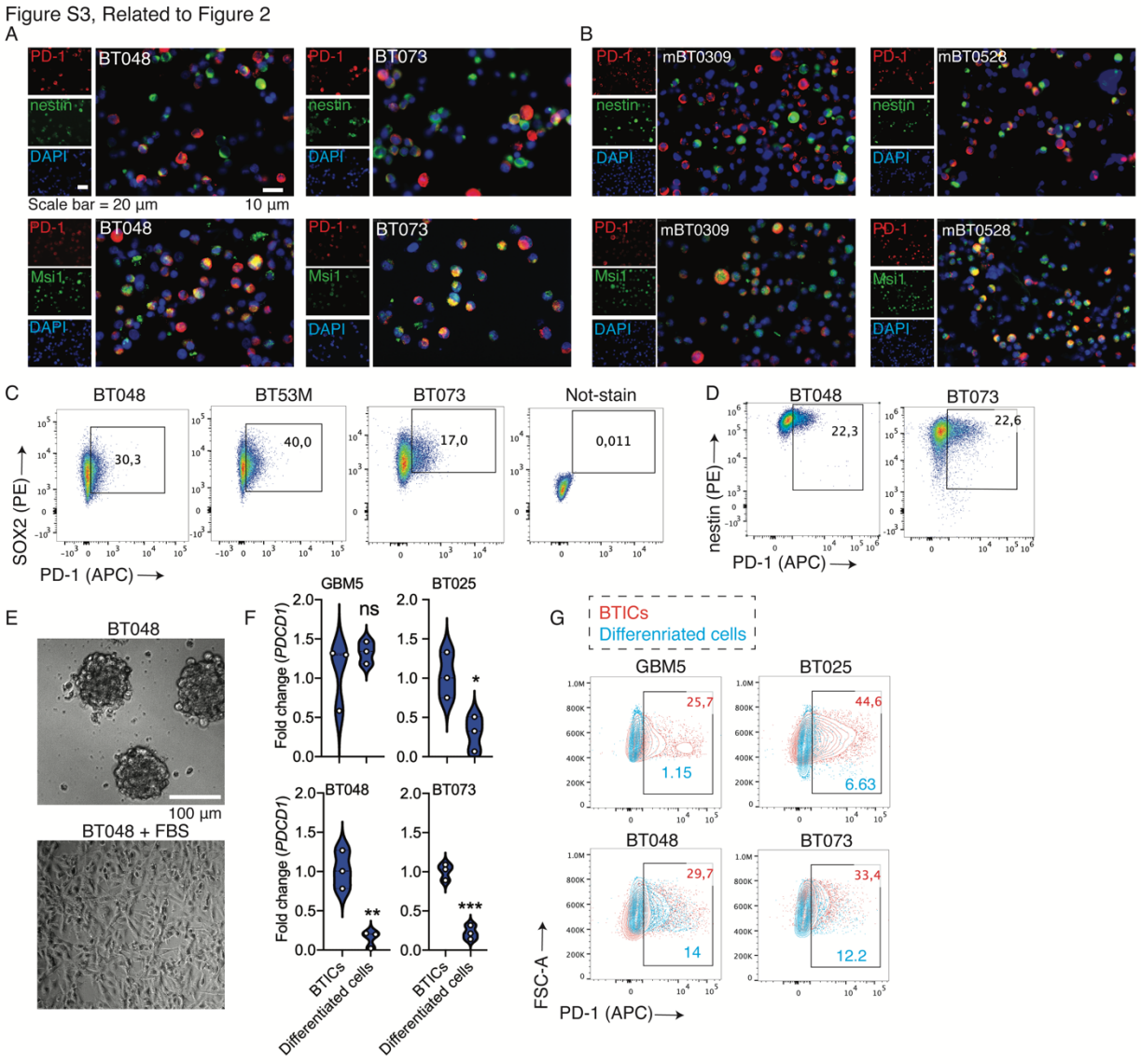

Fig. S3. The coexpression of PD-1 and stemness markers on mouse and human BTIC lines, Related to Fig. 2. (A, B) Immunofluorescence images of human and mouse BTIC lines double stained for PD-1 and BTIC markers musashi1 (Msi1) or nestin. Nuclei were counterstained with DAPI. (C, D) Representative flow cytometry plots of co-expression of PD-1 and stemness marker SOX2 or nestin on patient-derived BTIC lines. (E) Images of BTICs taken using a brightfield microscope before and one week after they were exposed to 1% fetal bovine serum (FBS). (F) RT-qPCR analysis of

PDCD1 mRNA expression in differentiated cells compared with undifferentiated counterparts of four human BTIC lines. (G) Flow cytometry plots of PD-1 expression in differentiated cells versus undifferentiated counterparts of four human BTIC lines. All images and graphs representative of 2-3 separate experiments. Means were compared by Unpaired [two-tailed] t test, *$p < 0.05$, **$p < 0.01$, ***$p < 0.001$, ****$p < 0.0001$. ns, not significant. Data are represented as mean ± SEM.

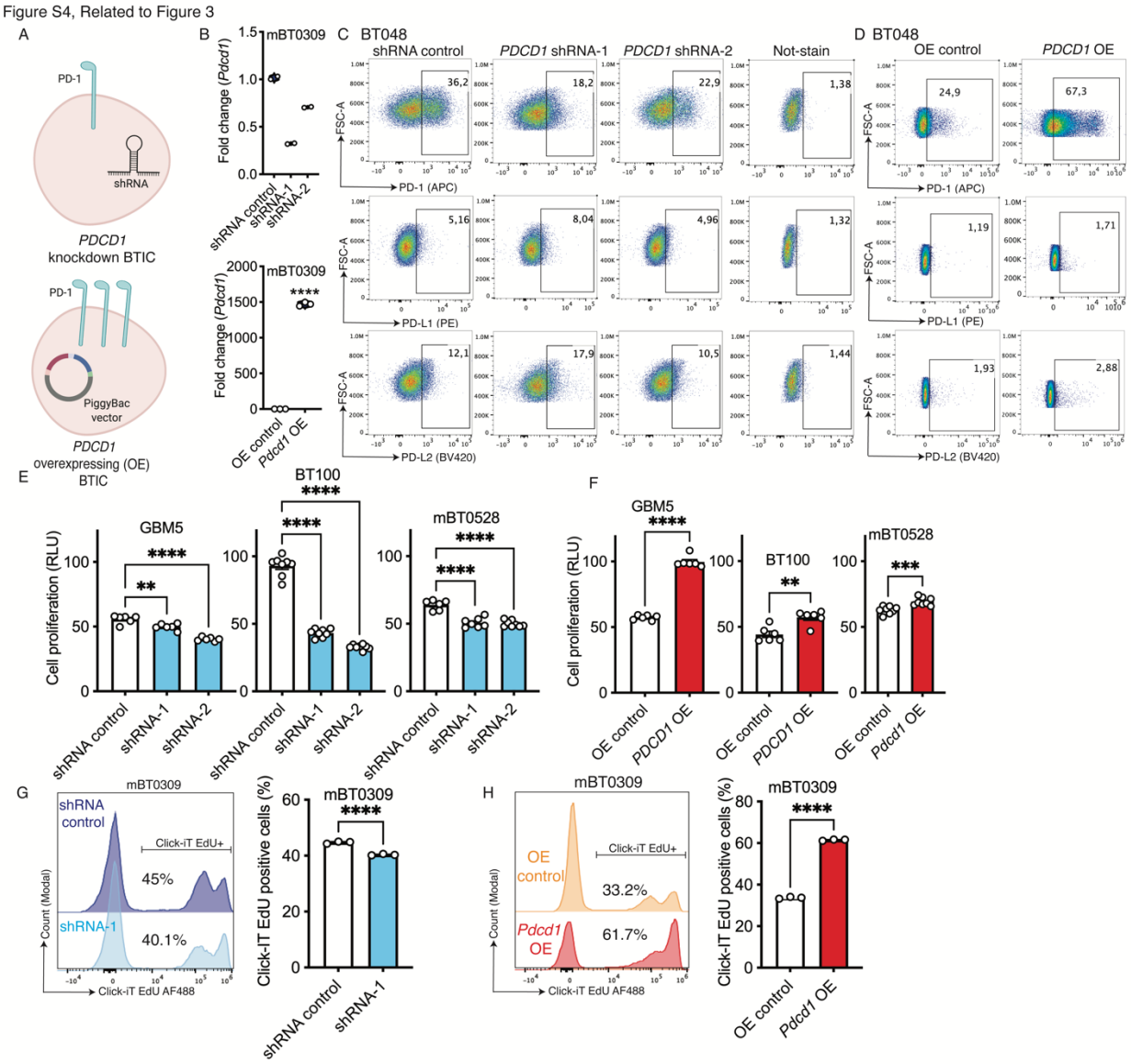

Fig. S4. PD-1 expression by BTICs promotes BTIC growth, Related to Fig. 3. (A) Schematic of generation of stable *PDCD1* knockdown or overexpressing (OE) BTIC lines by shRNAs in lentiviral vector and *PDCD1* encoding constructs in PiggyBac (PB) vector, respectively. Cells transduced with non-target shRNA plasmid or transfected with PiggyBac plasmid were used as controls for knockdown (shRNA control) or overexpressing (OE control) BTICs, respectively. (B) RT-qPCR analysis of *Pdcd1* expression in mouse BT0309 transfected with downregulating or overexpressing

vectors. Fold changes were calculated relative to *Pdcd1* expression in respective vector controls and normalized to *Gapdh* expression. (C, D) Flow cytometry study of PD-1, PD-L1 and PD-L2 expression on BT048 following PD-1 downregulation or overexpression compared to vector controls. (E, F) Human (GBM5 and BT100) and mouse (BT0528) BTIC lines with PD-1 downregulation or overexpression were compared to respective vector controls in a luminescence ATP proliferation assay. (G, H) Proliferation of a mouse BTIC line with PD-1 downregulation or overexpression measured by detecting EdU incorporation into DNA during the S phase of the cell cycle. Data representative of 2-3 separate experiments. Means were compared to respective vector control by unpaired [two-tailed] t test when comparing two groups. For more than two groups, one-way ANOVA with Tukey's post hoc was used. $^{**}p < 0.01$, $^{***}p < 0.001$, $^{****}p < 0.0001$. Data are represented as mean ± SEM

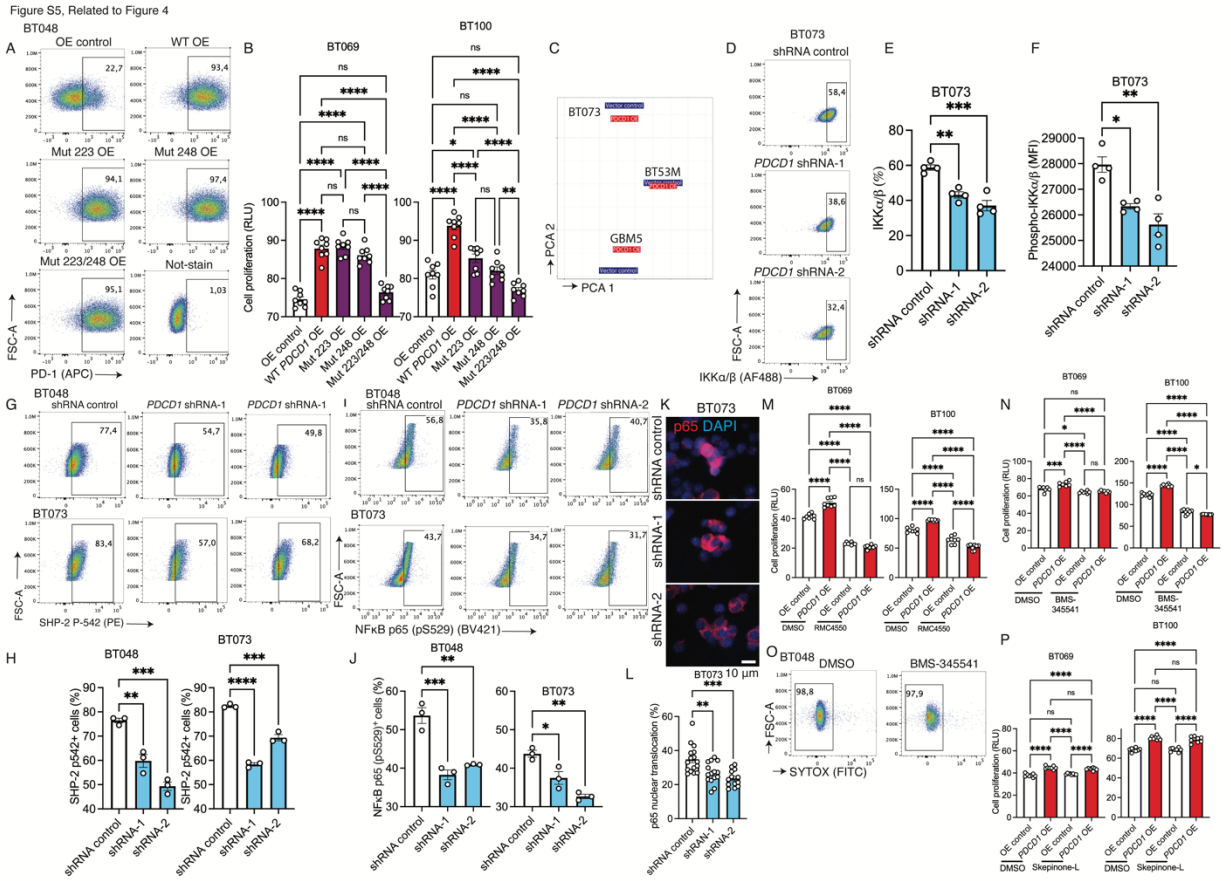

Fig. S5. PD-1 signaling in BTICs activates NFκB pathway, Related to Fig. 4. (A) Flow cytometry plots of PD-1 expression in BT048 transfected with overexpressing vectors encoding wild-type (WT), 223, 248 or 223/248 mutant (Mut) version of PD-1 compared to OE control. (B) ATP proliferation assay of human BT069 and BT100 cells overexpressing WT or mutant versions of PD-1 compared with OE control. (C) Principal components analysis of RNA-seq data of *PDCD1*-overexpressing cells versus OE control of three human BTIC lines. (D) Representative flow cytometry and bar plots of total IKKα/β expression in *PDCD1*-downregulated BTICs versus shRNA control. Alexa Fluor 488 (AF488) labelled antibodies were used to stain the cells. (F) Flow cytometry analysis of phosphorylation of serine residue 176/180 of IKKα or serine residue 177/181 of IKKβ (Phospho-IKKα/β) in *PDCD1*-downregulated BTICs versus shRNA control. MFI:

Mean fluorescence intensity. (G, H) Flow cytometry and bar plots of SHP-2 phosphorylation at tyrosine 542 in human BT048 and BT073 where PD-1 is downregulated by two distinct shRNAs compared with shRNA control. (I, J) Representative flow cytometry and bar plots of phosphorylation at serine residue 529 (pS529) of p65 subunit NFκB transcription factor. (K, L) Analysis of p65 nuclear translocation by immunofluorescence cell staining of *PDCD1*-downregulated BT073 versus shRNA control. For each well of cells, 4 field of views (FOVs) were imaged for quantitative analysis. Luminescence ATP proliferation test of *PDCD1*-overexpressing BT069 and BT100 cells compared to OE controls after 72 hours of treatment with (M) SHP-2 inhibitor RMC4550 (3 Mμ) or (N) IKKα/β inhibitor BMS-345541 (1 Mμ). (O) Representative flow cytometry plots of viability assay of BT048 treated with IKKα/β selective inhibitor BMS-345541 (1 μM) for 72 hours. Control cells were treated with dimethyl sulfoxide (DMSO). Dead cells were labeled with SYTOX green nucleic acid stain. (P) ATP proliferation assay of *PDCD1*-overexpressing BT069 and BT100 cells compared to OE controls after 72 hours of treatment with p38-MAPK inhibitor Skepinone-L (1 Mμ). Results are representative of n = 2-3 independent experiments. One-way ANOVA with Tukey's post hoc was used to compare means across groups. *p < 0.05, **p < 0.01, ***p < 0.001, ****p < 0.0001. ns, not significant. Data are represented as mean ± SEM

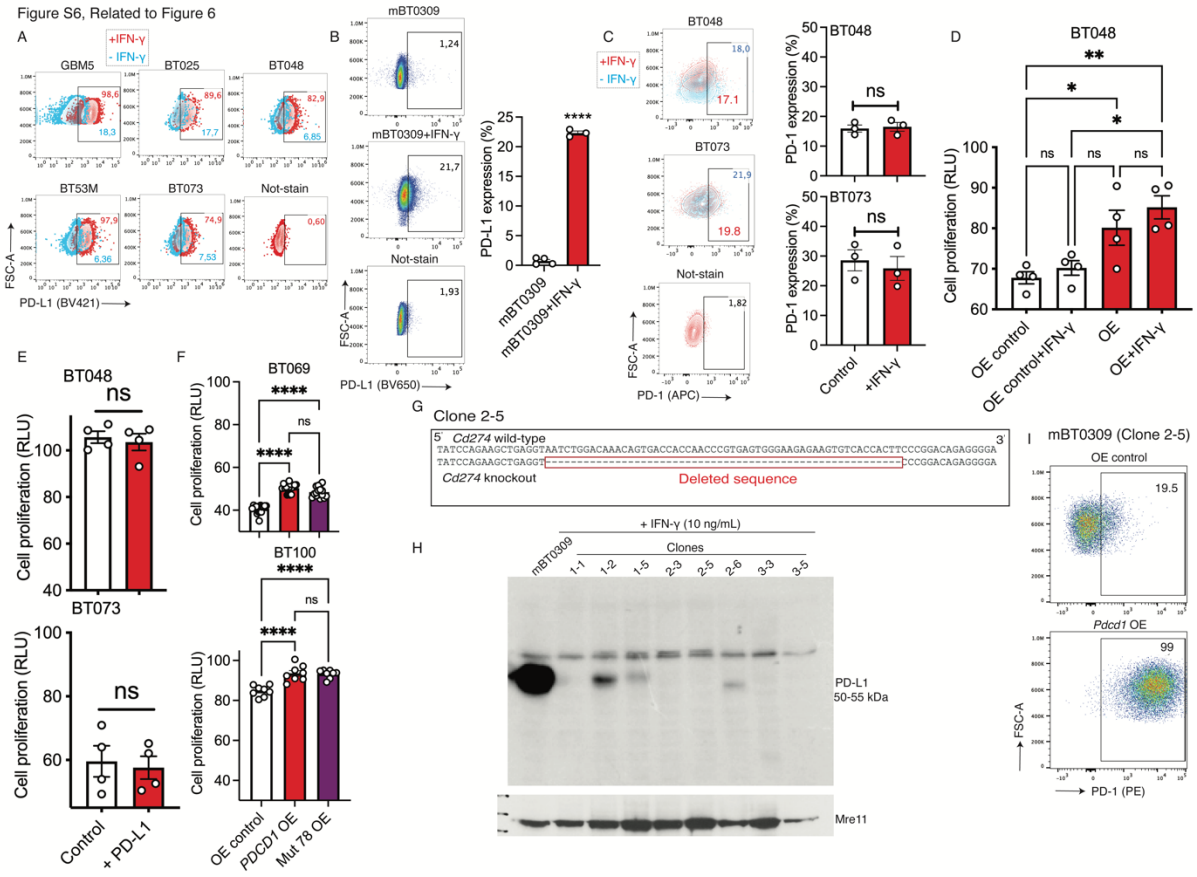

Fig. S6. BTIC-intrinsic PD-1 independent of PD-L1 ligation promotes tumor growth, Related to Fig. 6. (A) Representative flow cytometry plots of PD-L1 expression on five human BTIC lines after exposing cells to recombinant IFN-γ (10 ng/mL) for 48 hours. (B) Flow cytometry and bar graphs of surface PD-L1 expression on mouse BT0309 following treatment with recombinant IFN- (10 ng/mL). (C) Representative flow cytometry and bar plots of surface PD-1 expression on human BTIC lines BT048 and BT073 after treatment with IFN-γ. (D) Luminescence ATP proliferation assay of OE control and *PDCD1*-OE BT048 following treatment with IFN-γ for 48 hours. (E) Luminescence ATP proliferation assay of wild-type BT048 and BT073 in the presence or absence of 5 μg/mL recombinant human PD-L1 Fc. (F) ATP proliferation assay of two human BTIC lines overexpressing wild-type or mutant version of PD-1 (K78A)

compared to OE control. (G) Sequence of genomic DNA around short guide RNA site in clone 2-5 of mBT0309. Red box shows deleted sequence. (H) Western blot analysis of PD-L1 expression in different clones of *Cd274* knockout mBT0309 generated by CRISPR/Cas9 gene editing system. Cells were treated with IFN-γ before protein extraction. Mre11 was used as a loading control. Experiment conducted once. (I) Flow cytometry plots of PD-1 expression in mBT0309 after transfecting *Cd274*-KO cells with *Pdcd1*-OE vector. Means were compared to respective control by unpaired [two-tailed] t test when comparing two groups. For more than two groups, one-way ANOVA with Tukey's post hoc was used, *$p < 0.05$, **$p < 0.01$, ****$p < 0.0001$. ns, not significant. All plots and graphs representative of 2-3 separate experiments unless otherwise stated. Data are represented as mean ± SEM

Table S1. Patient characterization of specimens resected from clinical samples

Patient	IDH	EGFR	PTEN	MGMT	New or rec*	Gender	Age (year)
101029	Wild type	Wild type	Mutant	Unmethylated	New	Male	78
101220	Wild type	Wild type	Mutant	Unmethylated	New	Male	60
100819	Wild type	Mutant	Mutant	Unmethylated	New	Male	54
110907	Wild type	Wild type	Wild type	Unknown	AO†	Female	56
110512	Wild type	Mutant	Mutant	Partially methylated	New	Male	59
1085	Wild type	Wild type	Unknown	Unknown	New	Unknown	Unknown
026-1	Wild type	Wild type	Unknown	Unknown	New	Unknown	Unknown

*Recurrent; †Anaplastic oligodendroglioma

Table S2. Identification of a panel of patient derived BTICs

BTIC	IDH1	EGFR1	PTEN	P53	MGMT	New or rec	Treatment	Gender	Age (year)
GBM5	Wild type	Wild type	Mutant	Mutant	Unmethylated	New	Unknown	Unknown	70
BT025	Wild type	Wild type	Mutant	Mutant	M/U*	New	Unknown	Male	57
BT048	Wild type	Mutant	Mutant	Wild type	Methylated	New	No	Male	68
BT53M	Wild type	Mutant	Wild type	Mutant	Methylated	New	Unknown	Male	59
BT073	Wild type	vIII†	Mutant	Mutant	Unmethylated	Unknown	Unknown	Male	52
BT069	Wild type	Het mutant	Mutant	Mutant	Unmethylated	New	No	Male	51
BT089	Wild type	Wild type	Wild type	Wild type	Methylated	New	RT§+TMZ¶	Female	60
BT100	Wild type	Wild type	Wild type	Wild type	Unmethylated	New	No	Male	63
BT169	Wild type	Wild type	Het mutant**	Mutant	Unknown	New	RT+TMZ	Male	41
BT238	Wild type	Mutant	Wild type	Wild type	Unmethylated	New	RT+TMZ	Male	61
BT2313	Wild type	Unknown	Unknown	Unknown	Unmethylated	New	Unknown	Male	68
BT2314	Wild type	Unknown	Unknown	Unknown	M/U	New	Unknown	Male	57

*Methylated/Unmethylated; †EGFR variant III; §Radiation therapy; ¶Temozolomide;
**Heterozygous mutant

Data file S1 (Microsoft Excel format). Differential gene expression in human BTIC lines overexpressing PD-1 versus control (raw data).